We are IntechOpen,
the world's leading publisher of
Open Access books
Built by scientists, for scientists

6,900
Open access books available

186,000
International authors and editors

200M
Downloads

Our authors are among the

154
Countries delivered to

TOP 1%
most cited scientists

12.2%
Contributors from top 500 universities

CLARIVATE ANALYTICS
BOOK CITATION INDEX
INDEXED

WEB OF SCIENCE™

Selection of our books indexed in the Book Citation Index
in Web of Science™ Core Collection (BKCI)

Interested in publishing with us?
Contact book.department@intechopen.com

Characteristics of an Ultra-Wideband (UWB) Butterfly-Shaped Monopole Antenna

Qiubo Ye[1], Zhi Ning Chen[2] and Terence S. P. See[2]
[1]Communications Research Centre
[2]Institute for Infocomm Research
[1]Canada
[2]Singapore

1. Introduction

UWB is a promising wireless technology that can operate at very low power emission levels while communicating high data rates over short distances. It has attracted much attention as a means of expanding capacity from the already heavily utilized wireless bands. The Federal Communications Commission (FCC) has allocated a bandwidth of 7.5 GHz between 3.1 GHz to 10.6 GHz for commercial UWB communication systems.

In this emerging technology, the antenna design is a challenge. Like conventional antenna design, the return loss has to remain higher than 10 dB over the frequency range of operation. For a UWB antenna, the radiation properties should be reasonably satisfactory over the bandwidth. For example, omni-directional radiation patterns are required for indoor and vehicular applications. For a more complete pattern analysis, the total field which includes the co- and cross-polarizations of the radiation should be taken into account. The time domain performance such as the group delay and impulse response should also be examined (Chen et al., 2004).

Recently, several monopoles have been proposed for various UWB applications. These antennas make use of different structures to meet the requirements of return loss and radiation pattern. A monopole comprised of a square planar structure positioned perpendicular to the ground plane has been proposed, where bevelling or a shorting post is used to optimize and achieve a broad impedance bandwidth (Ammann & Chen, 2003). A bi-arm rolled monopole (Chen, 2005) which is constructed by rolling a planar monopole has shown that it is capable of achieving broadband and omni-directional radiation characteristics within the UWB band. The UWB antenna in (Behdad & Sarabandi, 2005) consists of half of a coupled sectorial loop above the ground plane. The optimized design is able to achieve an 8.5 : 1 frequency bandwidth for the voltage standing wave ratio (VSWR) < 2.2. Its radiation patterns are relatively consistent within the frequency band. In another design (Liang et al., 2005), a printed circular disc monopole is fed by microstrip line. Its impedance bandwidth covers the UWB frequency band and the radiation patterns are nearly omni-directional. The antenna geometry in (Qiu et al., 2006) is a circular notched ring with an attached element inside the hole. This antenna has band-notched characteristics, which meet the input impedance requirement of the UWB band while avoiding interference

within the 5.15–5.875 GHz bands occupied by existing wireless systems. A half-bowtie radiating element with a staircase-shape and a modified ground plane has been proposed (Cho et al., 2006). It has a very wide impedance bandwidth and the wireless local area network (WLAN) band is notched in the vicinity of 5 GHz. The time domain performance of these monopoles has been investigated by simulation, measurement or both.

The antenna to be presented in this chapter consists of a butterfly-shaped monopole above a ground plane. The butterfly-shaped radiator comprises two circular or elliptical wings which are connected to the two edges of a conducting plate. The wings may make different angles with the ground plane. This antenna is designed to offer a 10-dB return loss across the entire UWB bandwidth. The radiation patterns and cross-polarization performance will be investigated by simulation and validated by measurement. In addition, the group delay is examined, and the transmitted and received signals are compared with two identical antennas placed at different angles relative to each other at a far-field separation.

This chapter is organized as follows. Section 2 describes the antenna configuration and design. A parametric study of the effect of the angle between the wings of the antenna and ground plane on the return loss $|S_{11}|$ is highlighted. Section 3 presents and analyzes the simulated and measured return losses and radiation patterns in detail. Section 4 examines the effect of the size of the ground plane on the antenna performance in terms of the return loss and radiation patterns. In Section 5, a two-antenna system is constructed to investigate the group delay as well as the characteristics of the transmitted and received signals. Finally, Section 6 concludes the chapter and points out possible future research directions in this area.

2. Antenna configuration and design

The proposed antenna is comprised of two perfectly electrically conducting (PEC) plates that are connected to the two edges of a rectangular PEC plate which is horizontal to the ground plane, as shown in Figure 1. The configuration mimics the shape of a butterfly. In general, the two PEC plates – two wings of the butterfly – can be circular, elliptical, or any shapes for impedance matching purpose. The antenna is implemented at a height h above the ground plane. In order to achieve the good impedance matching and desired radiation patterns, the angle α between the wing and the z-axis can be varied. The feed point of the antenna is located at its rectangular plate by a coaxial probe through a SubMiniature version A (SMA) connector.

In this chapter, the design with elliptical wings has been chosen and the effect of the angle α on the return loss is investigated. The antenna design starts with a conventional elliptical vertical monopole and an identical element is added for optimization. A conducting base is used to connect the two wings and feed cable. The optimized dimensions of the antenna are determined by simulation and shown as follows: The major axis of the elliptical wings $2b = 28.8$ mm, the minor axis $2a = 22.8$ mm, $w = 3$ mm, $h = 2$ mm, $l = 12$ mm, and $d = 5$ mm. Since the wavelength at 3 GHz (close to the lower edge operating frequency of 3.1 GHz) is 100 mm, the sizes of the major and minor axes of the elliptical wings are about a quarter of the wavelength.

Using Mentor Fidelity based on the FDTD method with $\alpha = 0°$, 15°, 30°, and 45°, the simulated return losses are displayed in Figure 2. It can be observed that when $\alpha = 0°$, 15°,
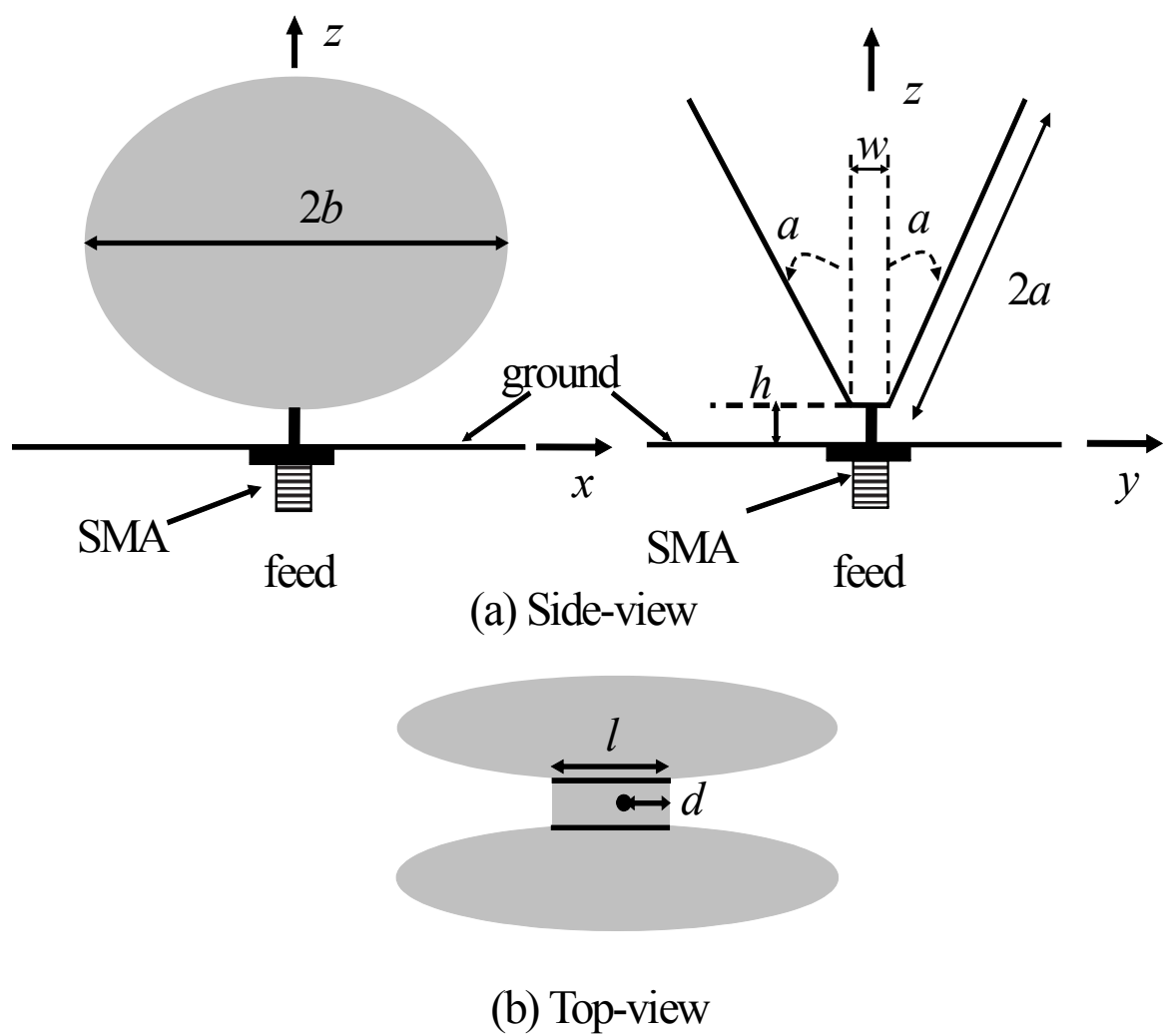
Fig. 1. Geometry of the butterfly-shaped antenna: (a) side-view; (b) top-view.

and 30°, the return loss $|S_{11}|$ is higher than 10 dB across the UWB band. The return loss bandwidth can be made much wider when α = 15° and 30° but the antenna height is lower as compared to the case when α = 0°. When α = 45°, the return loss $|S_{11}|$ is smaller than 10 dB between 3–4 GHz and 5–6 GHz. It can be concluded that the return loss will not be able to satisfy the UWB requirements when α > 45°. Therefore, it can be seen that the EM coupling between the two wings greatly affects the impedance matching of the antenna. With α greater than 45°, the wings get closer to the ground plane and the return loss will deteriorate because of the shorting effect by the ground plane. Compared to a conventional disc monopole, the antenna has one more degree of freedom for impedance matching. Since α can be varied over a certain range, the antenna can be designed with a lower profile in the vertical direction.

3. Analysis and discussion for return loss and radiation patterns

As a design example, the elliptical wings of the butterfly-shaped antenna are chosen to be orthogonal to the ground plane, i.e. α = 0° for ease of fabrication. The dimensions of the

antenna remain unchanged. This antenna was fabricated and verified by measurement. The first part of this section compares the simulated and measured return loss of the antenna. The second part provides the co- and cross-polarized radiation patterns at the two principal planes (*x-z* and *y-z*). The radiation patterns are displayed at three frequencies, 3, 7, and 10 GHz. For comparison, the simulated radiation patterns when $\alpha = 45°$ are added. The simulated co-polarized patterns of the antenna when $\alpha = 0°$ and $\alpha = 45°$ in the *x-y* plane at 3, 7, and 10 GHz are also shown. From the results, it can be concluded that the radiation patterns from 3 GHz to 10 GHz are generally stable and the radiation patterns are omni-directional in the azimuth (horizontal) plane.
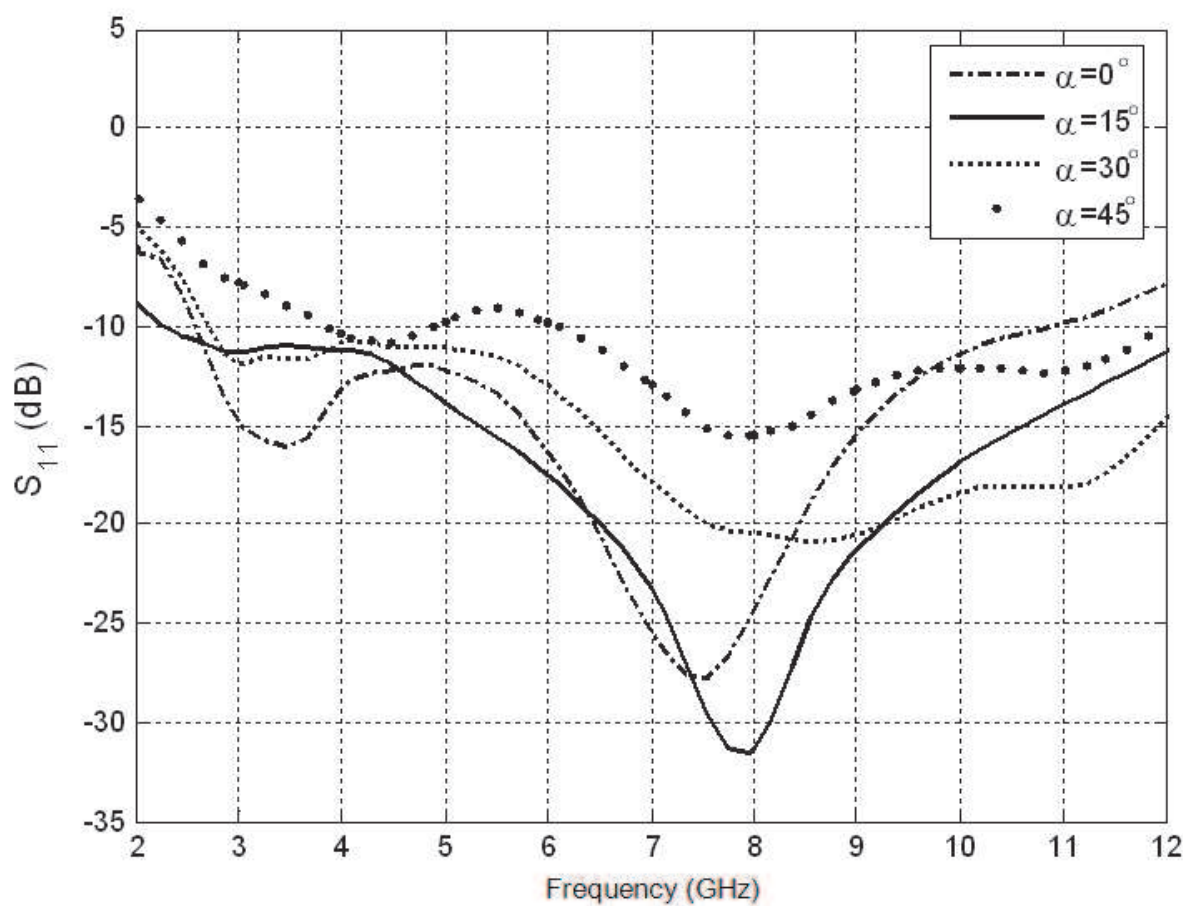
Fig. 2. Simulated return losses of the butterfly-shaped antenna for different angle α.

3.1 Return loss

The simulated and measured return losses $|S_{11}|$ are compared in Figure 3. The simulated return loss $|S_{11}|$ has a frequency range above 10 dB from 2.6–10.6 GHz, which covers the entire UWB band. On the other hand, the measured $|S_{11}|$ has a well-matched frequency range from 2.6–9.3 GHz. The slight discrepancy between the simulated and measured results at the higher frequency range is caused by the fabrication tolerance in that the antenna surfaces are not entirely flat and the two wings are not parallel at $\alpha = 0°$. This illustrates that the impedance matching is sensitive to the angle α.
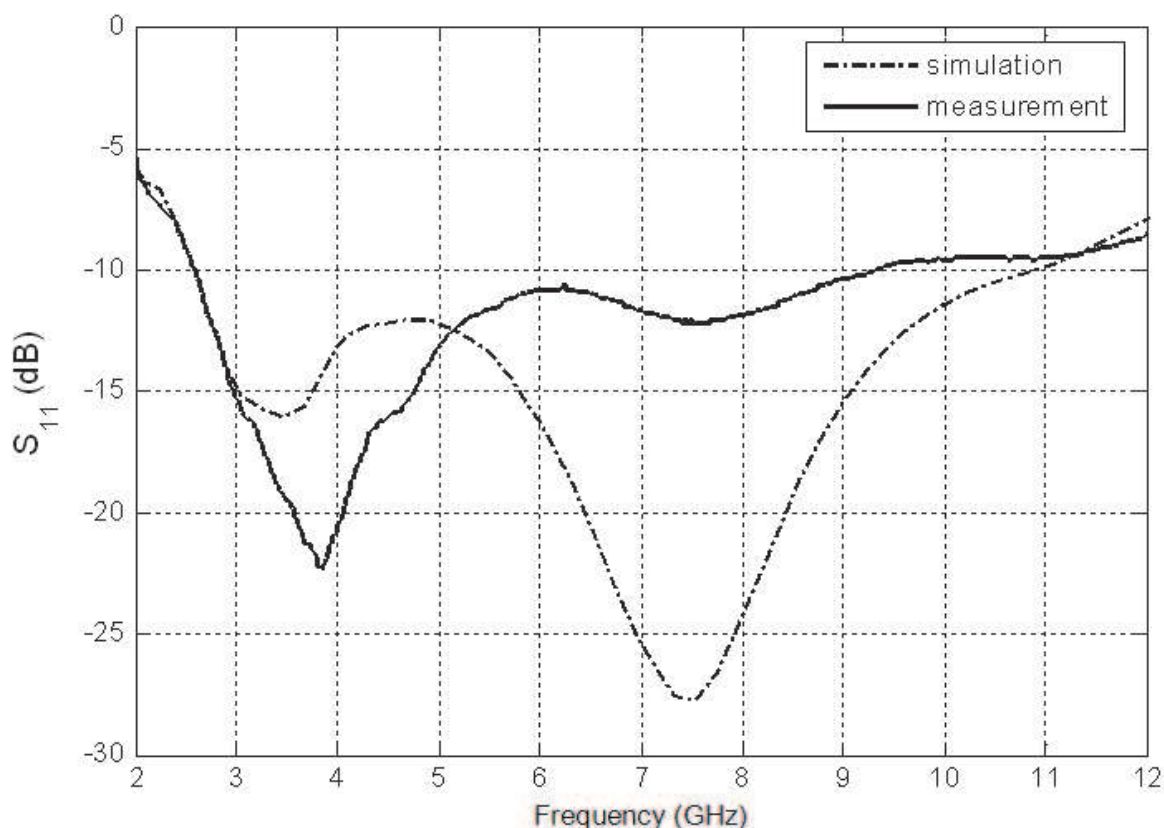
Fig. 3. Simulated and measured return losses.

3.2 Radiation patterns

Figures 4–6 show the co- and cross-polarized radiation patterns in the *x-z* plane at 3, 7, and 10 GHz, respectively. In the case when $\alpha = 0°$, both simulation and measurement results are displayed, and the simulated patterns when $\alpha = 45°$ are also given for comparison. It can be seen that the highest gain is around 5 dBi for the three frequencies. The ripples in the measured co-polarized radiation patterns are caused by the RF cable under the finite-size ground plane. Generally, good agreement between the simulated and measured co-polarized radiation patterns at the three frequencies has been achieved. The simulated cross-polarized radiation is typically below -40 dBi and the measured results are generally between -40 dBi and -15 dBi. This discrepancy is acceptable considering the difference in simulation and measurement setup. In the simulation, the SMA connector of the coaxial cable is not taken into account. Furthermore, it is difficult to get accurate data for levels below -30 dBi in the measurement. The simulated co-polarized patterns when $\alpha = 45°$ agree quite well with those when $\alpha = 0°$. Also, it can be observed that the gain is quite constant around 5 dBi for the three frequencies when $|\theta| = 50°$.
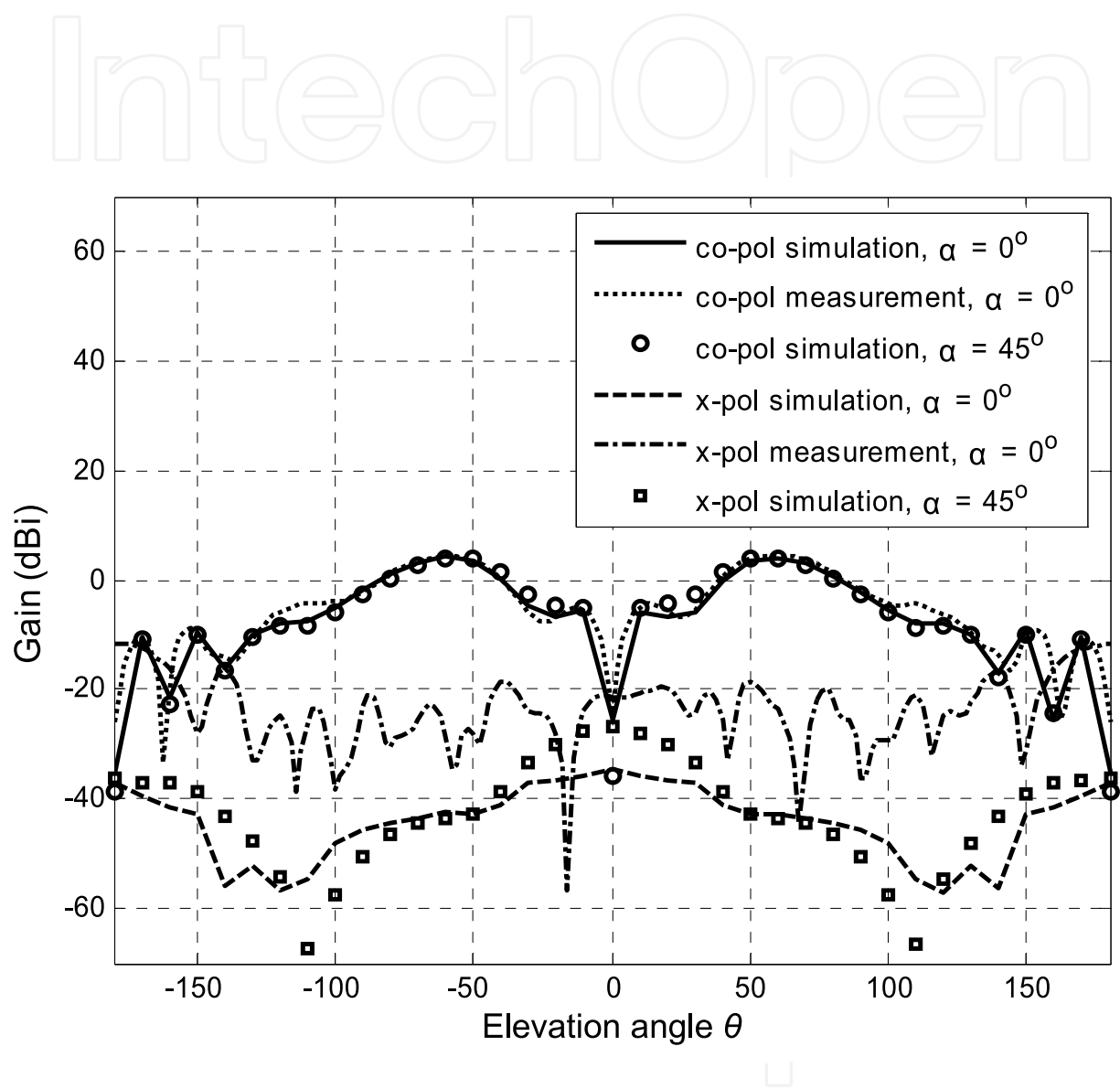
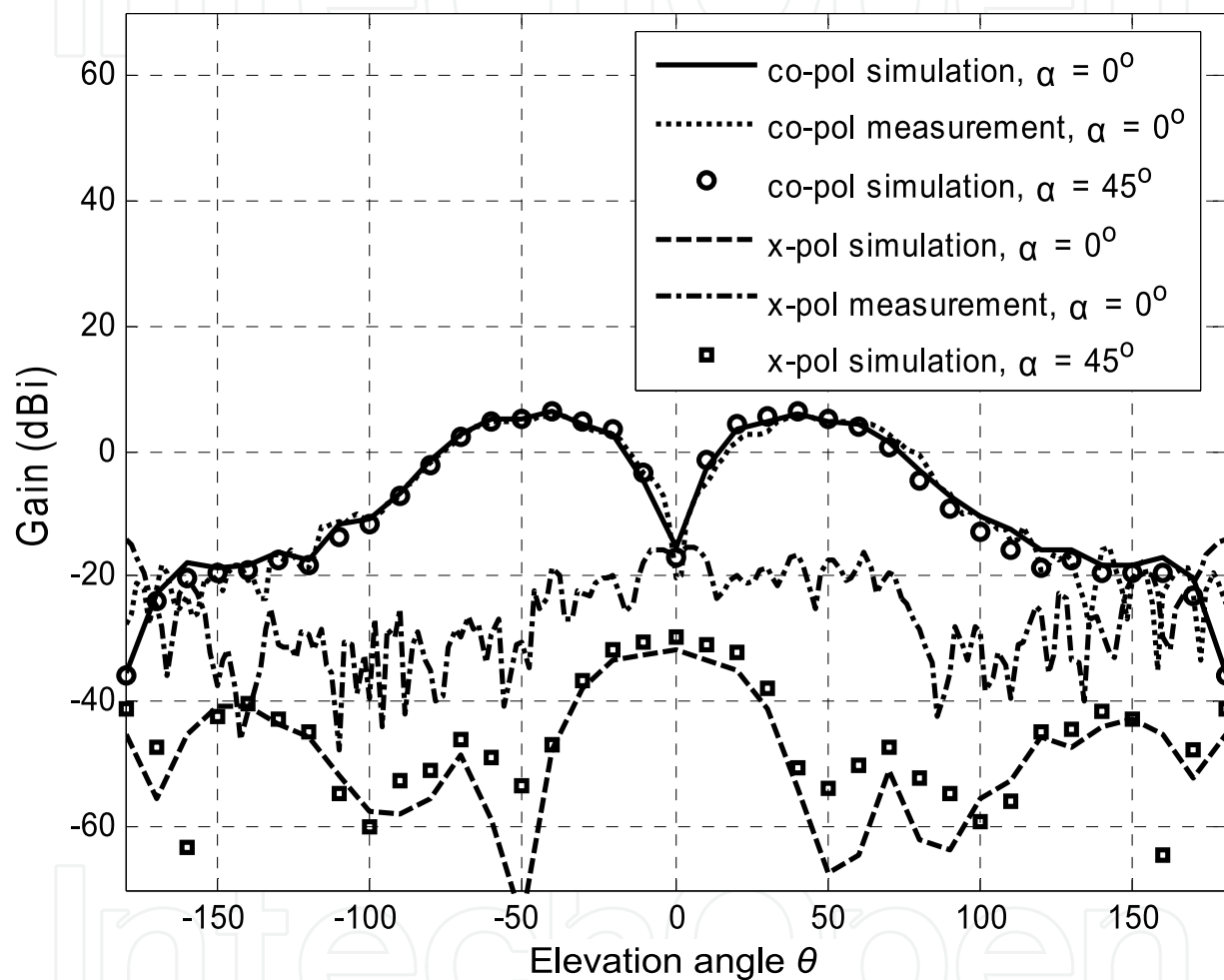Fig. 4. Radiation patterns in the *x-z* plane at 3 GHz.

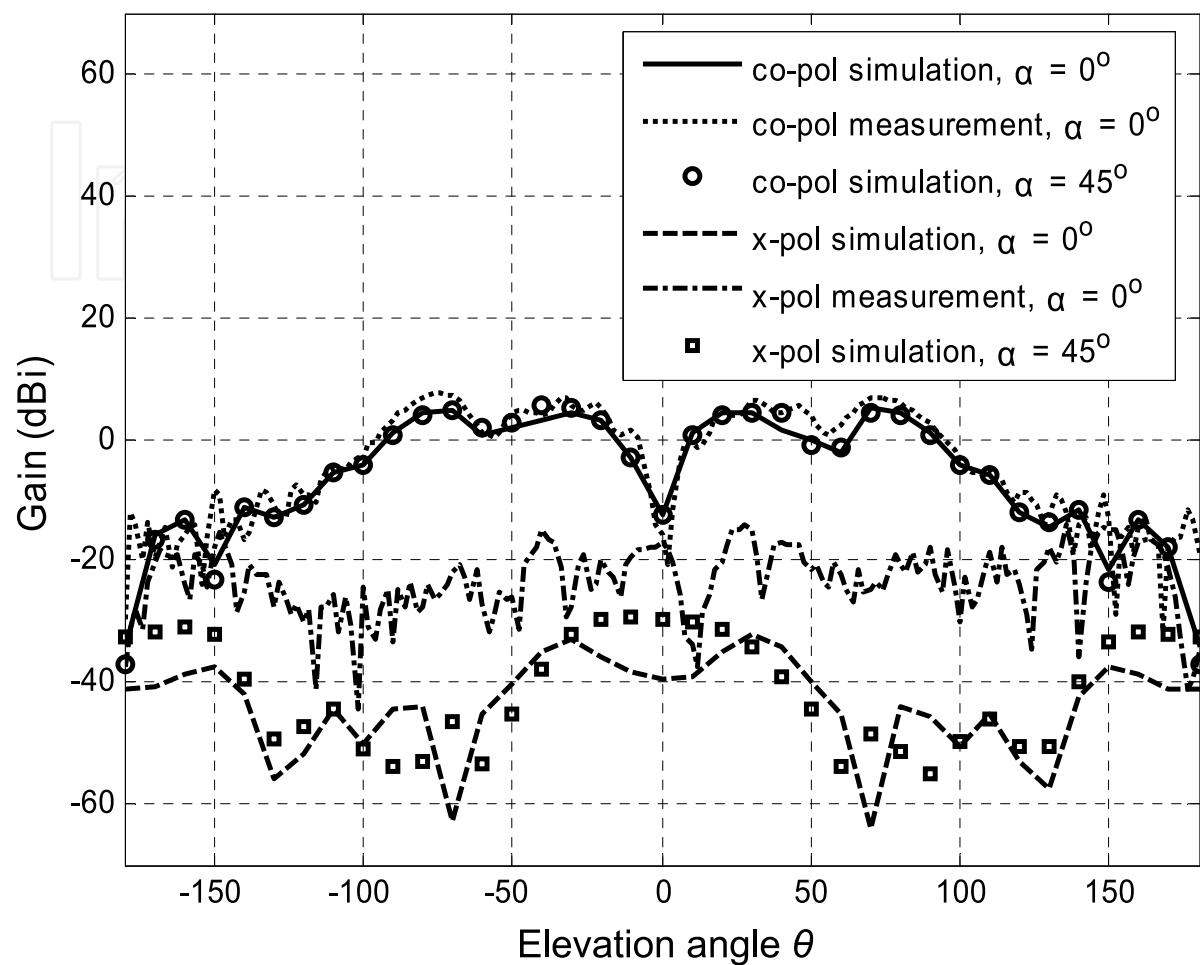Fig. 5. Radiation patterns in the *x-z* plane at 7 GHz.

Fig. 6. Radiation patterns in the *x-z* plane at 10 GHz.

Similarly, Figures 7–9 show the co- and cross-polarized radiation patterns in the *y-z* plane at 3, 7, and 10 GHz, respectively. In the case when $\alpha = 0°$, both simulation and measurement results are displayed, and the simulated patterns when $\alpha = 45°$ are also given for comparison. The highest gain is also around 5 dBi. Good agreement between the simulated and measured results for the co-polarized radiation patterns can be observed at 3 GHz and 7 GHz. At 10 GHz, the measured co-polarized gain is about 2 dBi higher than the simulated result. The measured cross-polarized pattern at 3 GHz is between -40 dBi to -20 dBi, while the simulated result is between -60 dBi to -25 dBi. At 7 GHz and 10 GHz, the simulated and measured cross-polarized patterns agree quite well. The simulated co-polarized patterns when $\alpha = 45°$ agree quite well with those when $\alpha = 0°$ at 3 GHz and 7 GHz but poorer agreement is observed in the co-polarized radiation patterns at 10 GHz. This is because the variation in the angle α has changed the radiation properties. The gain is quite constant around 5 dBi at the three frequencies when $|\theta| = 50°$. The small variation in the patterns is one of the factors to ensure that the waveform of the received signal is well-preserved.
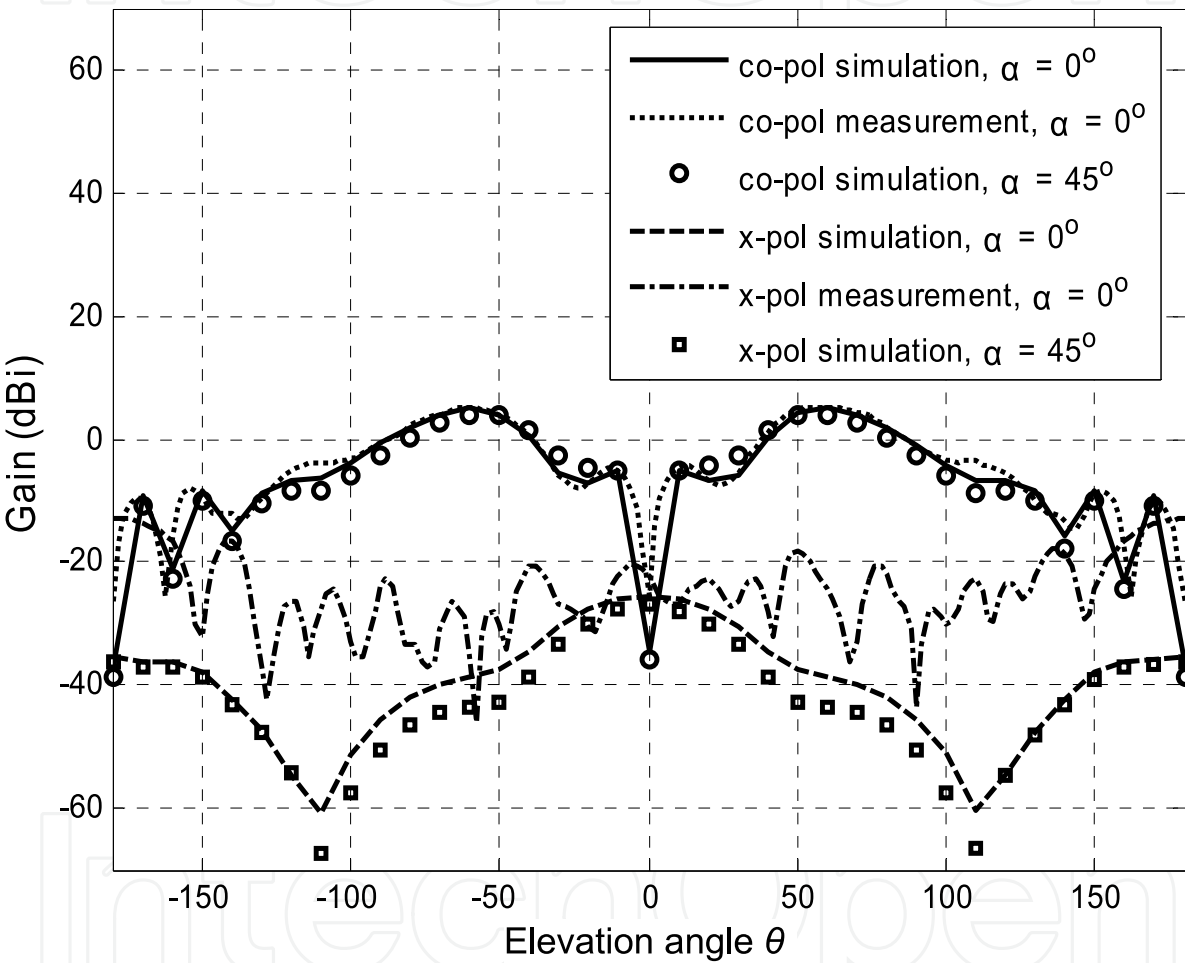
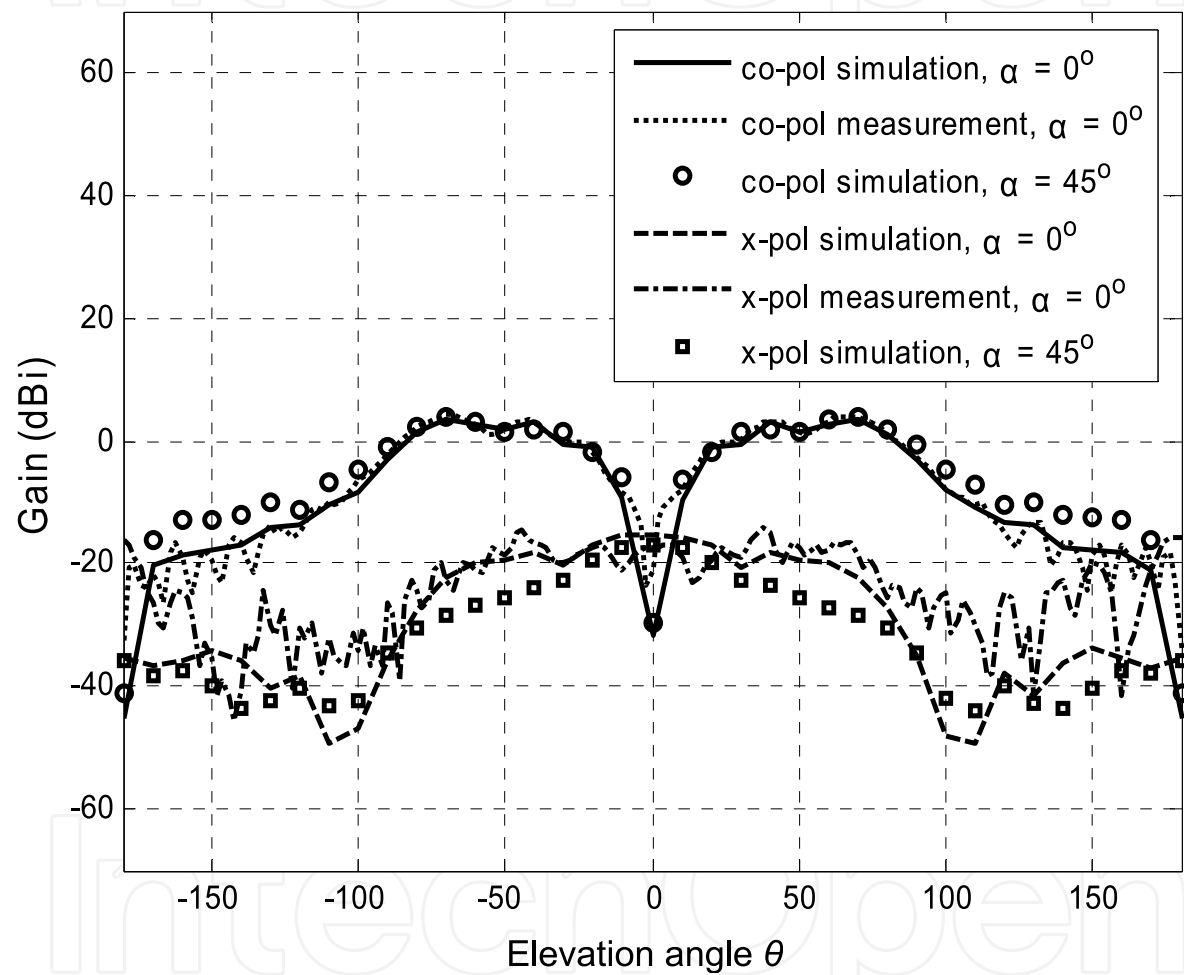Fig. 7. Radiation patterns in the *y-z* plane at 3 GHz.

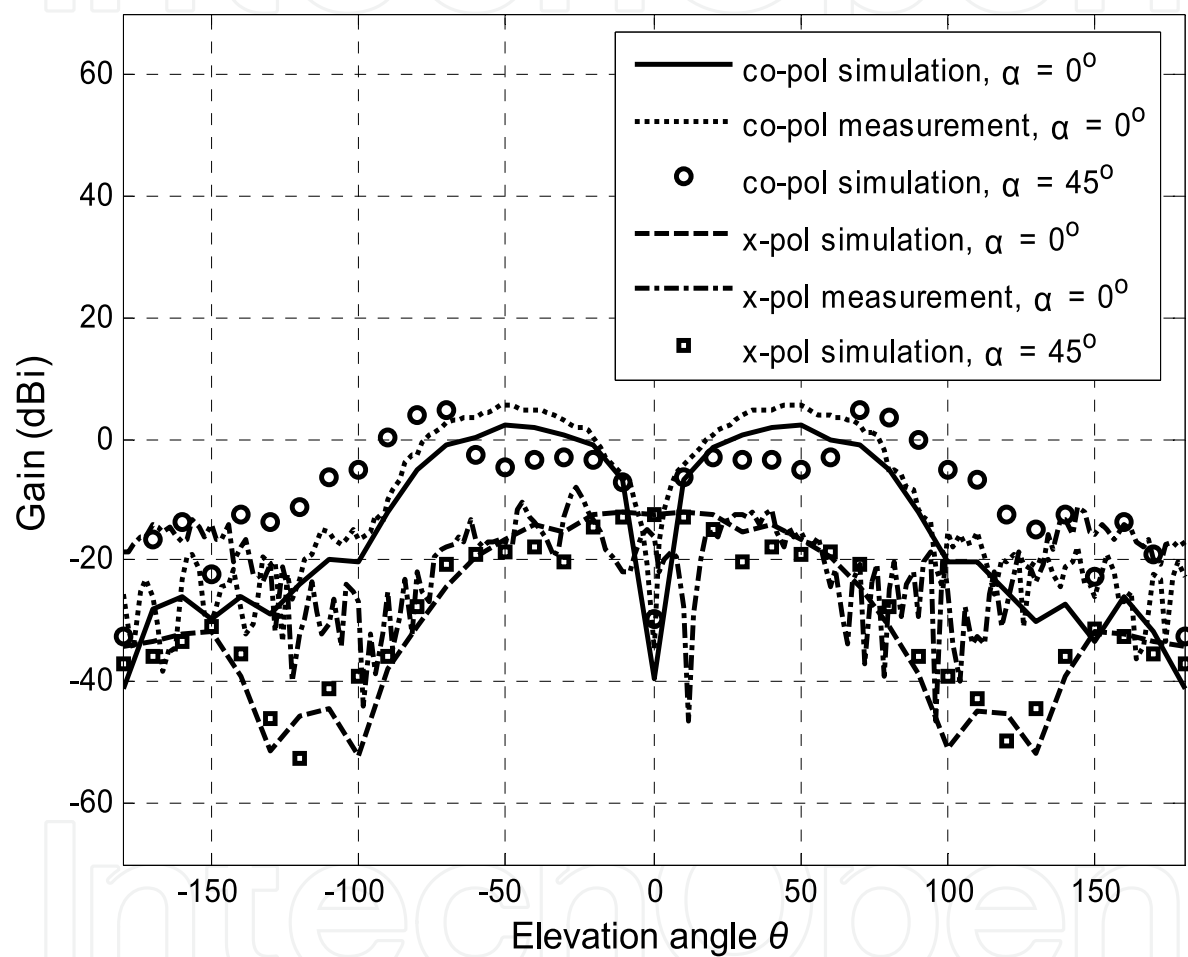Fig. 8. Radiation patterns in the *y-z* plane at 7 GHz.
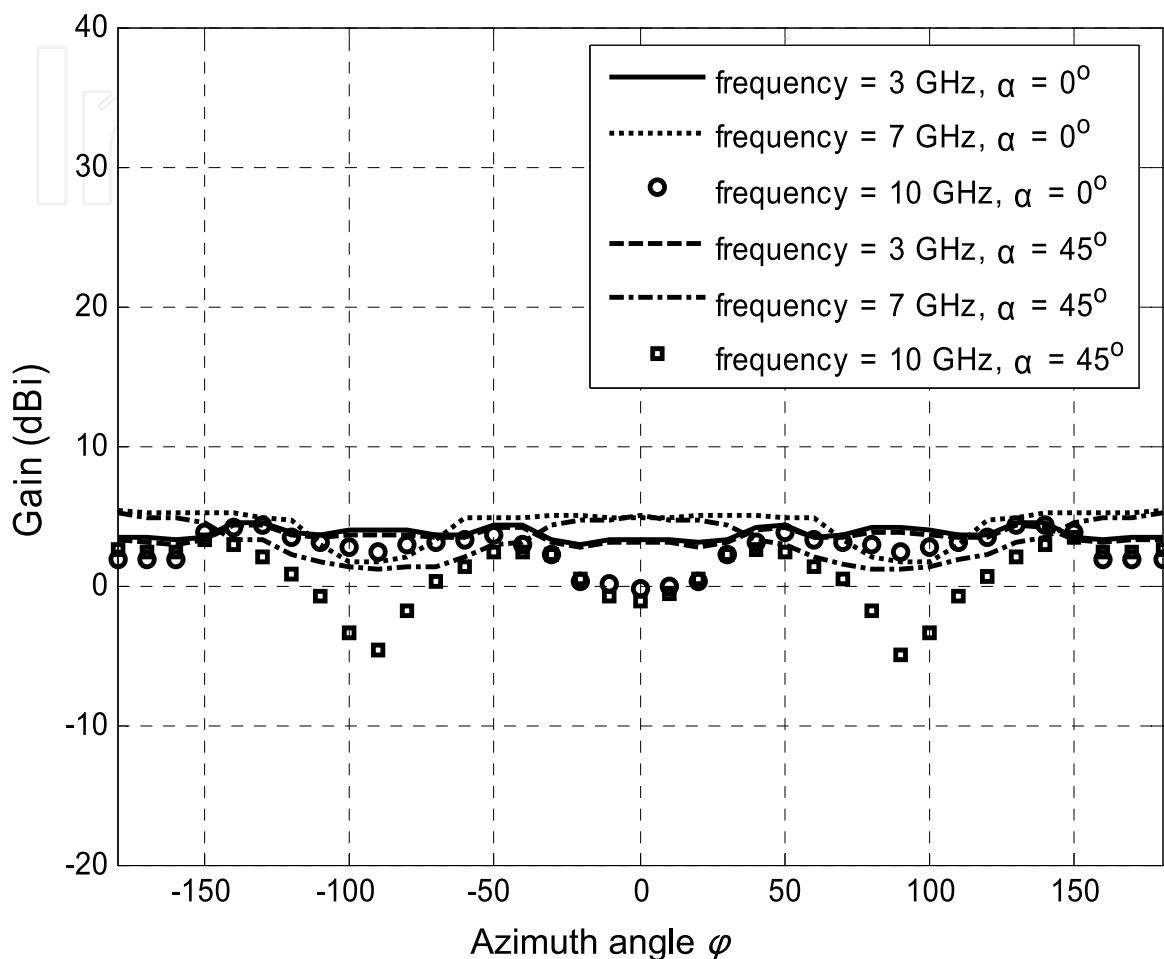
Fig. 9. Radiation patterns in the *y-z* plane at 10 GHz.

Fig. 10. Co-polarized radiation patterns in the *x-y* plane.

Figure 10 shows the simulated co-polarized patterns when $\alpha = 0°$ and $\alpha = 45°$ in the *x-y* plane at 3, 7, and 10 GHz. The radiation patterns are generally quite stable at the three frequencies, except for the case when $\alpha = 45°$ at 10 GHz.

From the radiation patterns in the *x-z, y-z,* and *x-y* planes, it can be concluded that the variation in radiation pattern from 3–10 GHz is small, giving omni-directional patterns in the azimuth plane. The small variation in the co-polarized radiation when α is changed from 0° to 45° is conducive for reducing the distortion in the received waveform (Chen et al., 2004).

4. Ground plane effect on the antenna performance

In the above discussions, the ground plane size for the antenna is 300 mm× 300 mm, which is much larger than the wavelength corresponding to the lower edge frequency of the UWB

band. Furthermore, depending on the requirements of different applications, the ground plane size for this antenna may be varied. From the study conducted in this Section, it will be shown that the size of the ground plane will greatly affect the antenna performance in terms of $|S_{11}|$ as well as the radiation properties such as gain, co- and cross-polarized radiation patterns across the bandwidth.

4.1 Ground plane effect on return loss

The FDTD-based Fidelity software from Mentor was used to investigate the performance of the antenna with different square ground planes of length 25, 50, 100, 200, and 300 mm.

The return loss performance for the antennas with different ground plane sizes is displayed in Figure 11. It can be observed that for ground plane sizes larger than 100 mm × 100 mm, the return loss is quite stable with little variation. When the size is reduced to 50 mm × 50 mm and then to 25 mm × 25 mm, the impedance matching deteriorates at the lower frequencies but remains relatively unchanged at the higher frequencies. Hence, the impedance bandwidth is reduced. This is expected because for the radiating elements of a monopole mounted on a finite-size ground plane, the outer edge of the ground plane diffracts the incident radiation in all directions. This diffraction consequently alters the current distribution on the ground plane. At 3 GHz, the ground plane size of 50 mm × 50 mm corresponds to ½ λ × ½ λ, and 25 mm × 25 mm is equivalent to ¼ λ × ¼ λ. When the ground plane size is reduced from 300 mm × 300 mm to 100 mm × 100 mm, the return loss remain almost unchanged. As the ground plane size is reduced to 50 mm × 50 mm, the return loss at 3 GHz increases by about 3 dB. When the ground plane size is further reduced to 25 mm × 25 mm, the return loss is increased by another 5 dB. Evidently, the outer-edge diffraction becomes increasingly significant as the size of the ground plane is reduced, especially when the size is less than 1 λ × 1 λ. With a small size, the edge diffraction adversely impacts the impedance matching of the antenna. The performance of the return loss at the upper edge of the frequency band is relatively unaffected as the size of the ground plane is still considered to be electrically large at the higher frequencies.

4.2 Ground plane effect on radiation patterns

The effect of the size of the ground plane on the radiation patterns has been investigated across the UWB band. Figures 12–14 show the simulated radiation patterns at 3.1 GHz, 6.85 GHz, and 10.6 GHz in the x-z plane. From Figure 12, it can be seen that for the small ground plane sizes of 25 mm × 25 mm and 50 mm × 50 mm, the patterns are quite flat across 40° < $|\theta|$ < 150° and the peak gain is close to 0 dBi. For the larger ground planes, the peak gain is greater than 0 dBi and peaks at around $|\theta|$ = 50°.

Figure 13 shows that the radiation patterns at 6.85 GHz peak at around $|\theta|$ = 50°. The peak gain is slightly higher than at 3.1 GHz. The antenna with a ground plane size of 25 mm × 25 mm experiences an increase in back lobes which can be reduced by increasing the size of the ground plane. From Figure 14, it can be observed that the ground plane size does not have a significant effect on the radiation patterns at 10.6 GHz, except for the higher back lobes when a smaller ground plane is used. In the main radiation directions, the gain varies from -3 dBi to 5 dBi across the bandwidth. Similar observations from the radiation patterns in the y-z plane can be made and are therefore not shown for brevity.
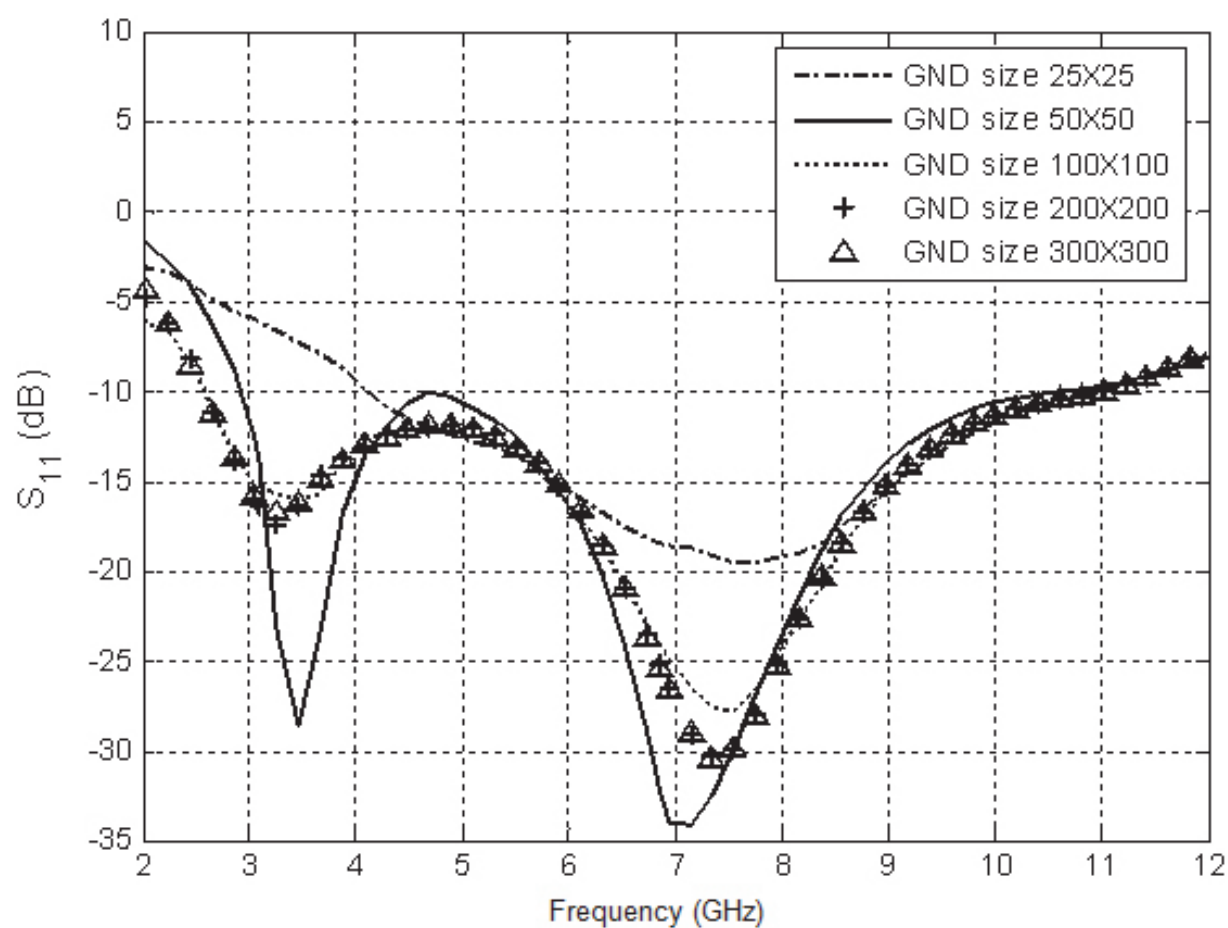
Fig. 11. Simulated return losses for the antennas with different ground plane sizes.

An infinite-size ground plane prevents monopole radiation into the half space beneath the ground plane. In practice, a monopole antenna has to be installed on a ground plane of finite size. It has been observed that the impedance matching will be degraded significantly if the ground plane size is smaller than $1\,\lambda \times 1\,\lambda$ as outer edge diffraction will modify the current distribution on the ground plane and the monopole antenna. The radiation characteristics of an antenna in terms of the gain and patterns will also be affected. This has been verified from Figures 12–14. At 3.1 GHz, the peak gain drops by about 5 dBi while the back lobe increases by approximately 5 dBi when the size of the ground plane is 50 mm × 50 mm and 25 mm × 25 mm. At 6.85 GHz, the peak gain drops by about 3 dBi and the back lobe is increased by approximately 5 dBi for the ground plane size of 25 mm × 25 mm as compared to other ground plane sizes. At 10.6 GHz, the back lobe is increased by approximately 6 dBi when the size of the ground plane is reduced to 25 mm × 25 mm. By decreasing the size of the ground plane, the magnitude of the currents along the outer edges of the ground plane is increased. Hence, the outer-edge diffraction effect becomes increasingly significant for antennas with small ground planes, which in turn alters the current distribution and thereby adversely affects the radiation properties by reducing the peak gain and increasing the back lobes.
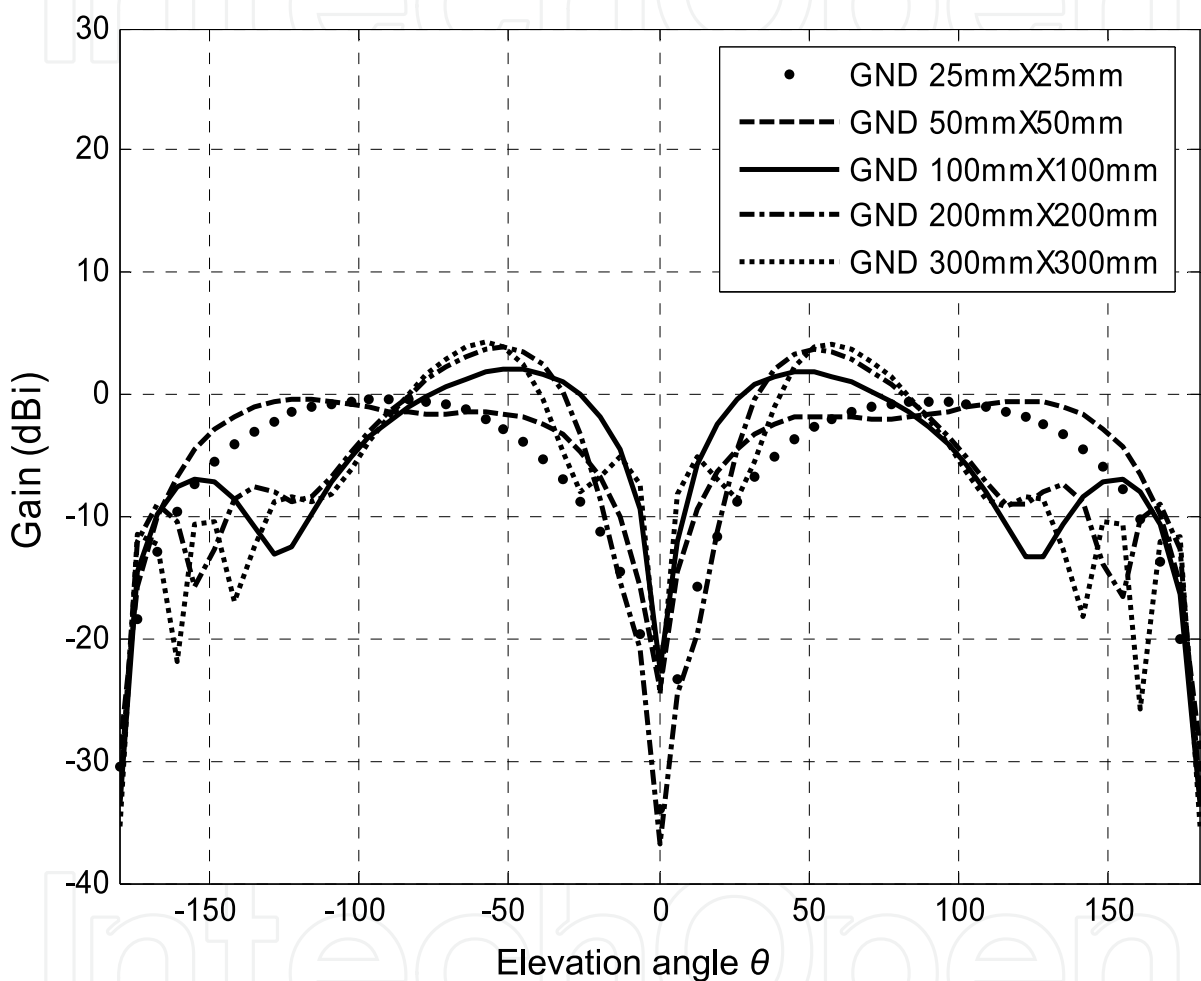
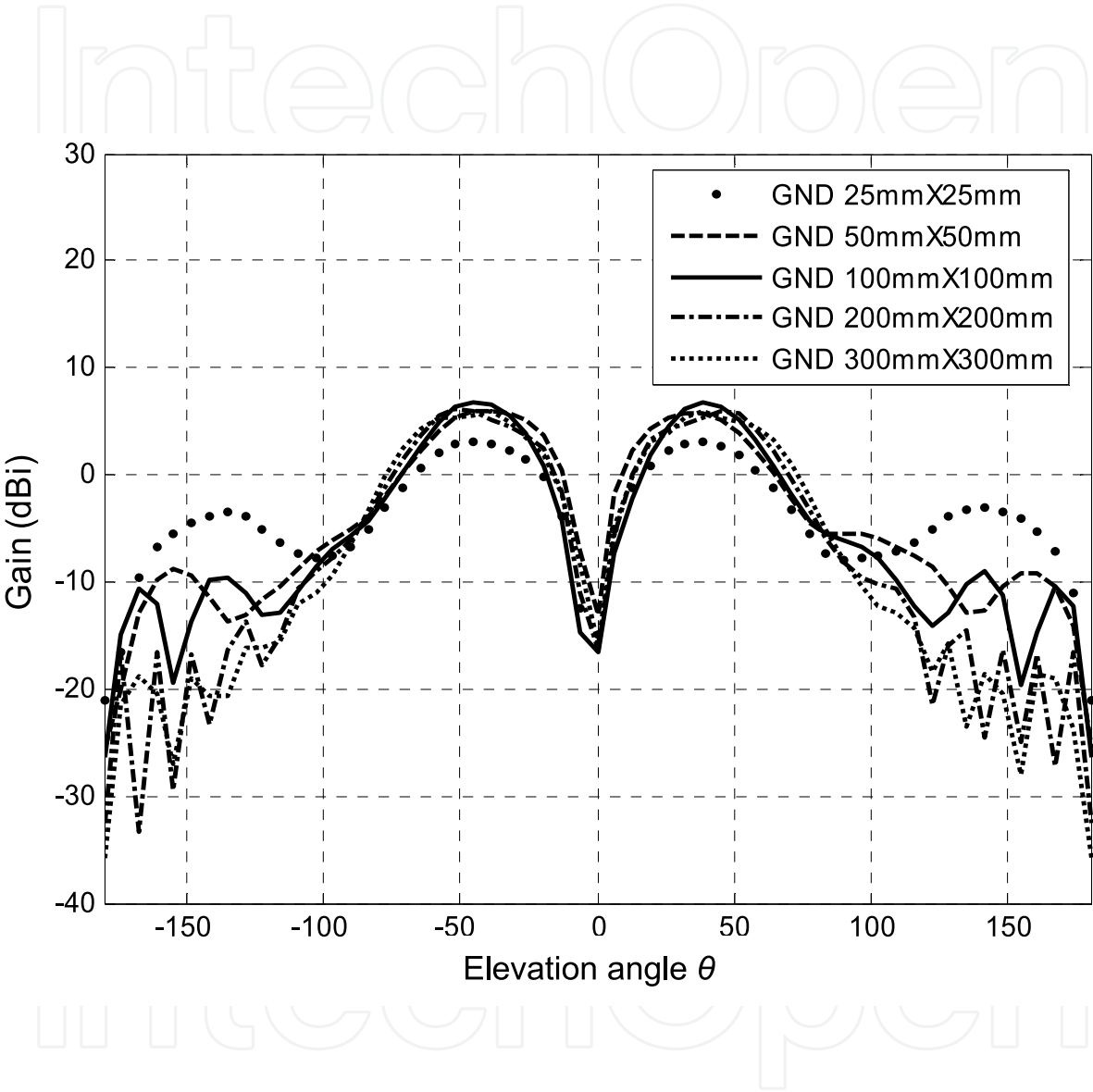Fig. 12. Simulated radiation patterns in the *x-z* plane at 3.1 GHz.

Fig. 13. Simulated radiation patterns in the *x-z* plane at 6.85 GHz.
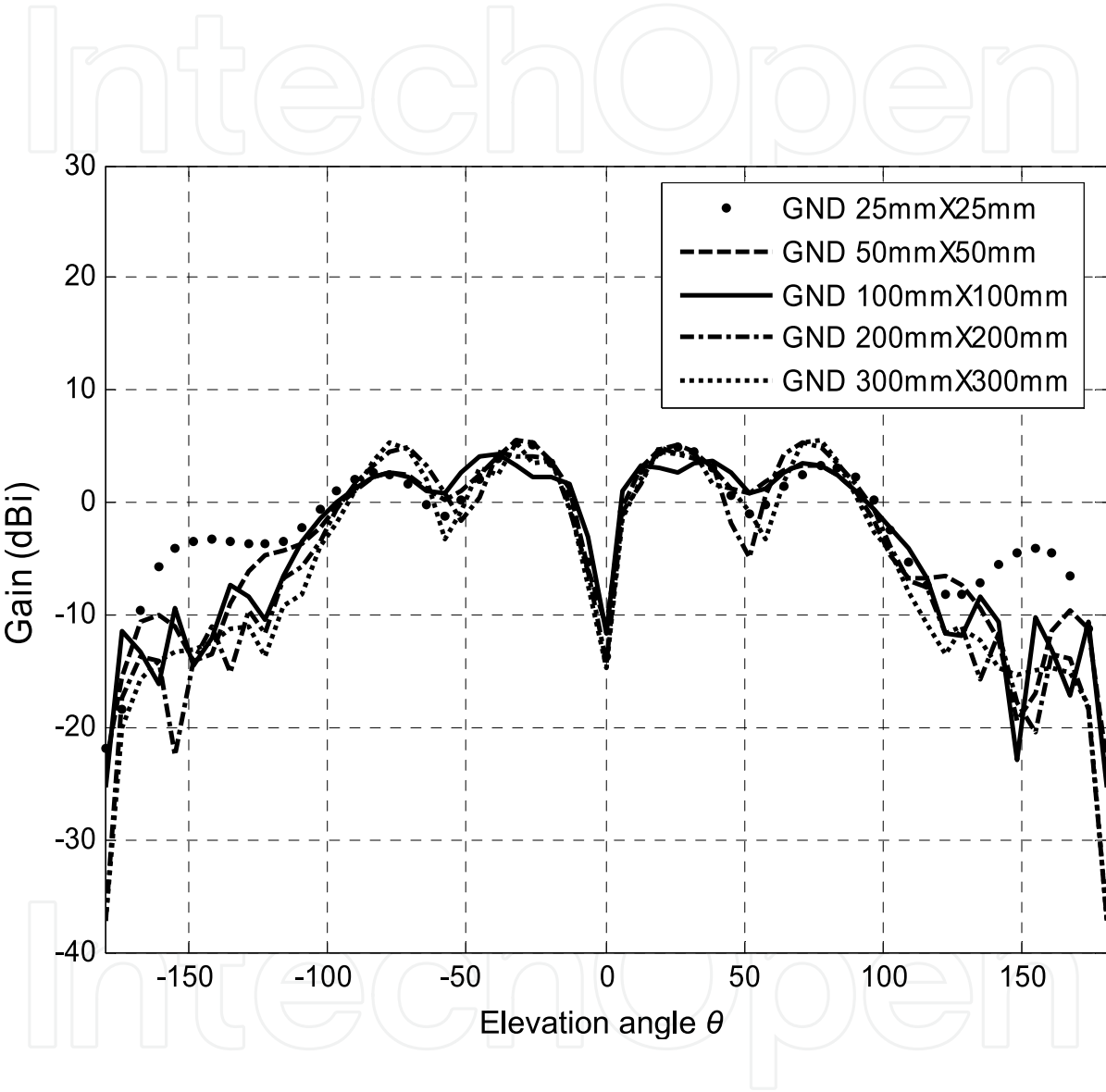
Fig. 14. Simulated radiation patterns in the *x-z* plane at 10.6 GHz.

5. Time domain characteristics

In order to evaluate the antenna performance in the time domain, a transmit-receive antenna system has been built. The antenna system consists of two identical antennas separated by a distance in the far-field region. This system is implemented using an FDTD model and becomes a two-port structure. The source pulse is fed to the input of the transmit antenna. The radiated pulse from the output of the transmit antenna travels in free space before entering the receive antenna. In this study, the antenna with $\alpha = 0°$ will be considered. The receive antenna can be rotated at different angles with respect to the transmit antenna and the received pulse will then be compared with the source and radiated pulses.

The antenna system has been simulated using the FDTD method and the group delay is calculated and shown in Figure 15. The far-field distance between the two antennas is 250 mm. In this case, the two antennas are positioned face-to-face. The group delay is defined as the change in the phase of the transmission response S_{21} with respect to the angular frequency and it provides information about the degree of signal distortion. From Figure 15, it can be seen that the variation in the group delay is within 1 ns within the UWB band. Beyond 11 GHz, the frequency components suffer from time distortion, which results in a reduced fidelity of the received signal.
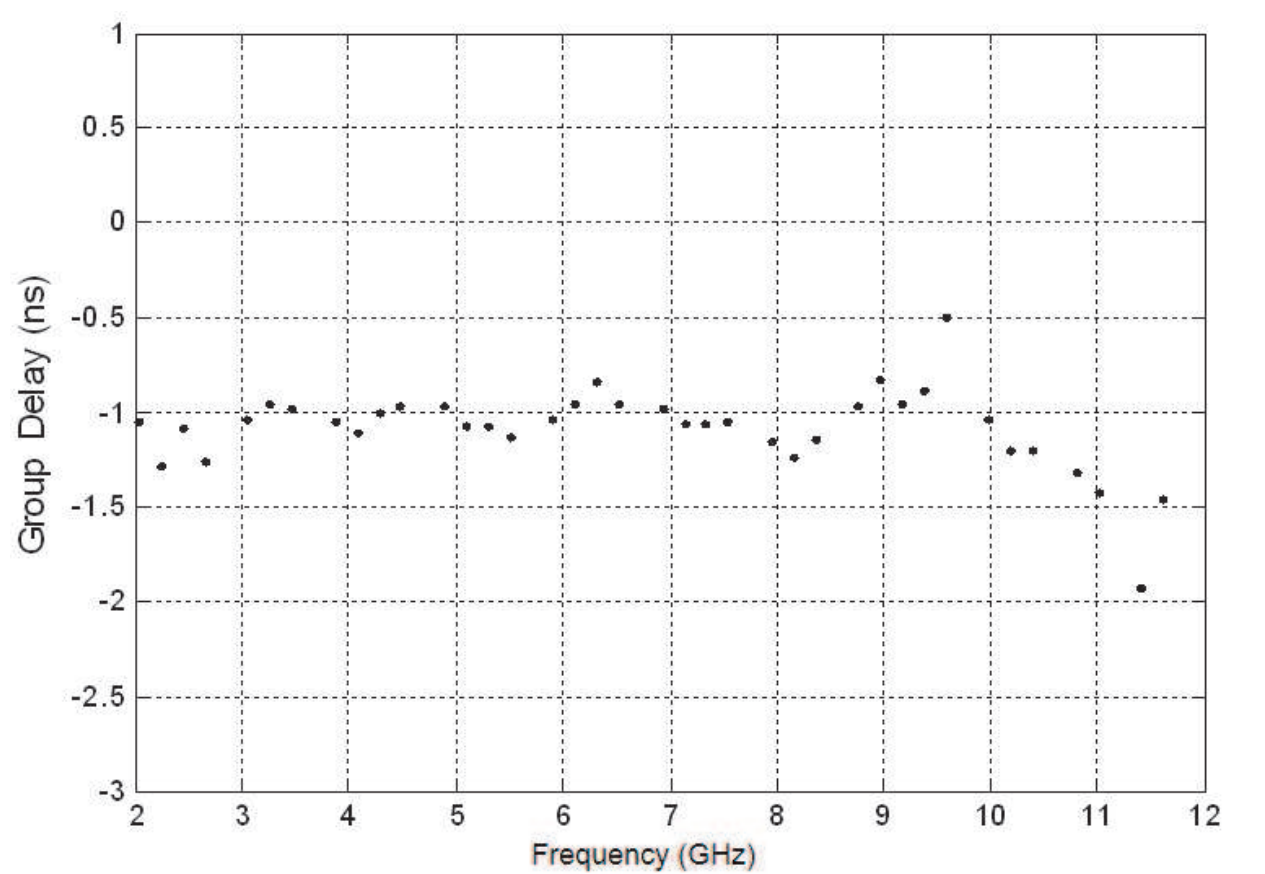

Fig. 15. Group delay of the antenna system.

Figure 16 shows the comparison of the received signals when the receive antenna is oriented at angles of 0°, 45°, and 90° with respect to the transmit antenna. The source and radiated pulses are also included. Rx 0° represents the received signal when the wings of the receive antenna are directly facing the wings of the transmit antenna, while Rx 90° represents the signal when the wings of receive antenna are perpendicular to the wings of the transmit antenna. All the received signals have been normalized with respect to the source pulse for comparison. It can be observed that the shapes of the received signals are similar and the normalized peak amplitude in the main lobe varies from 1 V to around 0.7 V for the different angles. The peak amplitude in the ripple of the received signals changes from around 0.1 V to 0.4 V. The distortion in the received signal may be caused by the larger variation in the group delay of the antenna system, especially at the higher frequencies.
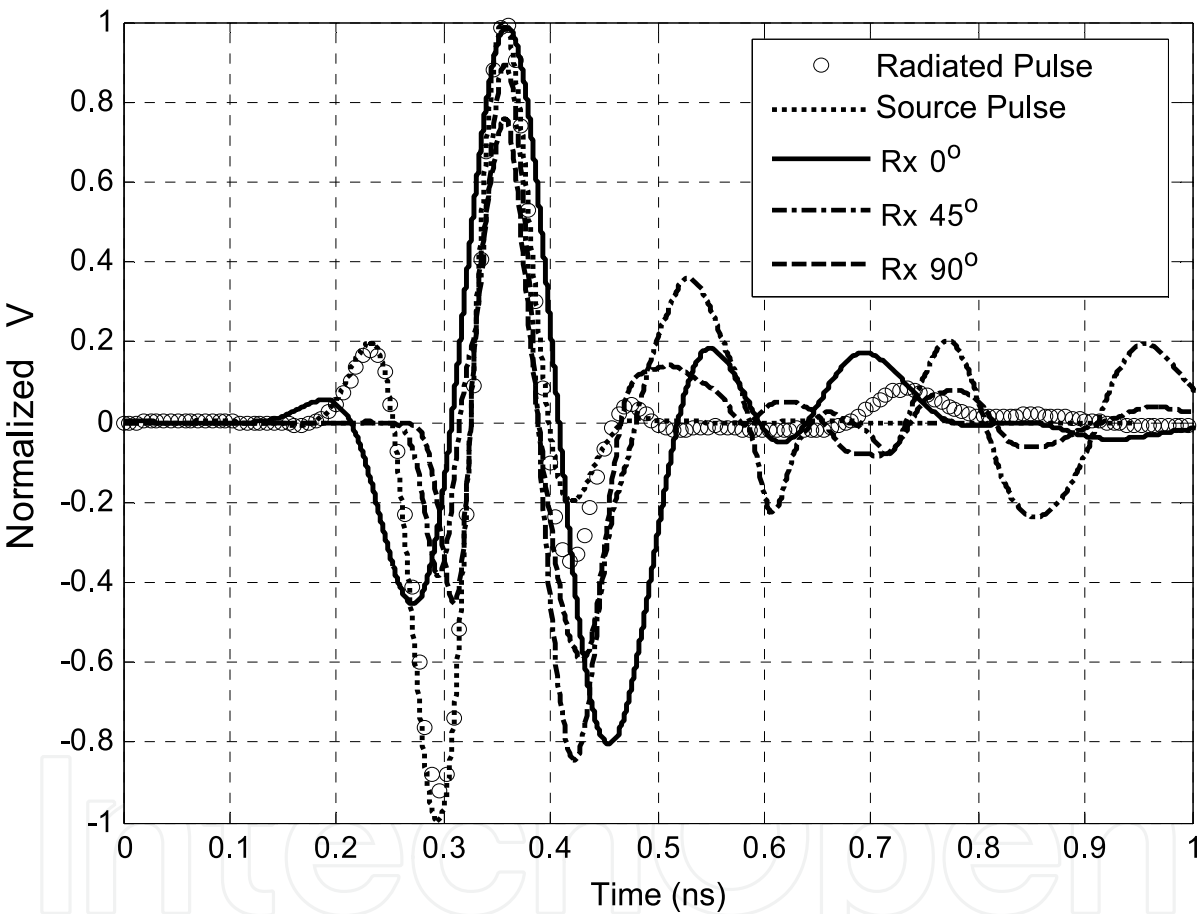

Fig. 16. Comparison of the received pulse with the source and radiated pulses.

6. Conclusion

The proposed butterfly-shaped monopole antenna has demonstrated good impedance and radiation performance across the UWB band. The wings of the antenna can be oriented at an angle of up to 45° with respect to the ground plane and still meet the UWB requirements. The co- and cross-polarized radiation patterns for the proposed antenna have shown stable performance across the entire UWB band in the principal planes. In addition, the radiation is omni-directional in the azimuth plane. However, at 10 GHz, the

patterns are adversely affected when $\alpha = 45°$. The design has been validated by both simulation and measurement.

A study has been conducted to investigate the effect of the size of the ground plane on the antenna performance. It has been shown that when the size of the ground plane is comparable to or smaller than $1\,\lambda \times 1\,\lambda$ (wavelength corresponding to the lower edge of the UWB band), the return loss performance deteriorates, especially at the lower edge of the UWB band. At the same time, the small ground plane has resulted in a decrease in the peak gain at 3 GHz and an increase in the back lobe radiation across the entire UWB band.

Based on the phase of the transmission response S_{21} of the antenna system, the variation in the calculated group delay is within 1 ns across the UWB band. The received signals for the different angles of the receive antenna with respect to the transmit antenna are similar in shape and their peak amplitudes vary within a small range. The study has shown that this antenna is capable of providing stable gain and little distortion in the radiated and received pulses, which makes it suitable for pulsed based UWB wireless communication and radar applications.

Future research directions in this area may involve antenna miniaturization as well as the optimization of the current distribution on the antenna so as to reduce signal distortion. In order to avoid interference with other existing communication systems, band notching will be required, which may be achieved in the proposed butterfly-shaped monopole antenna by cutting slots on the radiators.

7. References

Ammann, M. J. & Chen, Z. N. (2005). Wideband Monopole Antennas for Multiband Wireless System, *IEEE Antennas & Propagation Magazine,* Vol. 45, No. 2, (Apr. 2003), pp. , ISSN 1045-9243.

Behdad, N. & Sarabandi, K. (2005). A Compact Antenna for Ultrawide-Band Applications, *IEEE Transactions on Antennas and Propagation,* Vol. 53, No. 7, (Jul. 2005), pp. 2185-2192, ISSN 0018-926X.

Chen, Z. N. (2005). Novel Bi-Arm Rolled Monopole for UWB Applications, *IEEE Transactions on Antennas and Propagation,* Vol. 53, No. 2, (Feb. 2005), pp. 672-677, ISSN 0018-926X.

Chen, Z. N.; Wu, X. H.; Li, H. F.; Yang, N. & Chia, M. Y. W. (2004). Considerations for Source Pulses and Antennas in UWB Radio Systems, *IEEE Transactions on Antennas and Propagation,* Vol. 52, No. 7, (July 2004), pp. 1739-1748, ISSN 0018-926X.

Cho, Y. J.; Kim, K. H.; Choi, D. H.; Lee, S. S. & Park, S.-O. (2006) A Miniature UWB Planar Monopole Antenna with 5-GHz Band-Rejection Filter and the Time-Domain Characteristics, *IEEE Transactions on Antennas and Propagation,* Vol. 54, No. 5, (May 2006), pp. 1453-1460, ISSN 0018-926X.

Liang, J.; Chiau, C. C.; Chen, X. & Parini, C. G. (2005). Study of a Printed Circular Disc Monopole Antenna for UWB Systems, *IEEE Transactions on Antennas and Propagation,* Vol. 53, No. 11, (Nov. 2005), pp. 3500-3504, ISSN 0018-926X.

Qiu, J.; Du, Z.; Lu, J. & Gong, K. (2006). A Planar Monopole Antenna Design with Band-Notched Characteristic, *IEEE Transactions on Antennas and Propagation,* Vol. 54, No. 1, (Jan. 2006), pp. 288-292, ISSN 0018-926X.
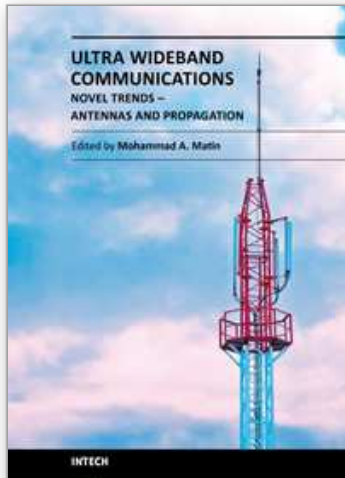
This book explores both the state-of-the-art and the latest achievements in UWB antennas and propagation. It has taken a theoretical and experimental approach to some extent, which is more useful to the reader. The book highlights the unique design issues which put the reader in good pace to be able to understand more advanced research.

How to reference

In order to correctly reference this scholarly work, feel free to copy and paste the following:

Qiubo Ye, Zhi Ning Chen and Terence S. P. See (2011). Characteristics of an Ultra-Wideband (UWB) Butterfly-Shaped Monopole Antenna, Ultra Wideband Communications: Novel Trends - Antennas and Propagation, Dr. Mohammad Matin (Ed.), ISBN: 978-953-307-452-8, InTech, Available from: http://www.intechopen.com/books/ultra-wideband-communications-novel-trends-antennas-and-propagation/characteristics-of-an-ultra-wideband-uwb-butterfly-shaped-monopole-antenna

INTECH
open science | open minds